Kazimierz JAKUBIUK, Maciej CZYŻAK, Robert SMYK, Mirosław WOŁOSZYN

Politechnika Gdańska, Katedra Elektrotechniki Teoretycznej i Informatyki

Measurement of magnetic signals of vehicles with denoising by matched filtering with FPGA FFT processor

Abstract*.The work describes the sensor subsystem for the magnetic signals of vehicles based on measuring the magnetic flux density as well as denoising unit. For this purpose a set of wireless magnetic sensors is used that allows to monitor the movement of vehicles at airports, seaports and border check-points. The measured signalls serve for detection and identification of vehicles. Since every vehicle is built of ferromagnetic components it perturbs the uniformity of the Earth magnetic field. This perturbation can be measured with the use of fluxgate sensors. In order to improve the signal-to-noise ratio the differential setting of the sensorsand the matched filtering based on the FFT FPGA core are applied. Such approach makes easier the detection and identification of objects. In this work the measurement subsystem, the realization of the matched filter based on the FFT FPGA processor and the results of simulation and experimental research are presented.*

Streszczenie. *W artykule przedstawiono podsystem czujników do pomiaru sygnałów magnetycznych od pojazdów, oparty na pomiarze indukcji magnetycznej. Do tego celu zastosowano zestaw czujników magnetycznych pracujących bezprzewodowo, który pozwala na monitorowanie ruchu pojazdów na lotniskach, w portach i punktach kontroli granicznej. Mierzone sygnały pozwalają na wykrywanie i identyfikację pojazdów. Ze względu na fakt, że każdy pojazd jest zbudowany z elementów ferromagnetycznych, które zaburzają pole magnetyczne Ziemi, zaburzenie to można zmierzyć przy zastosowaniu trójosiowych magnetometrów transduktorowych. W celu poprawienia stosunku sygnału do szumu zastosowano pomiar różnicowy i filtrację dopasowaną zrealizowaną w oparciu o procesor wykorzystujący jądro FFT w układzie FPGA. Takie podejście ułatwia wykrywanie i identyfikację obiektów. W pracy opisano system pomiarowy, realizację filtru dopasowanego wykorzystującego procesor FFT oraz rezultaty symulacji i badań eksperymentalnych* (***Pomiar sygnałów magnetycznych od pojazdów z odszumianiem wspomaganym filtracją dopasowaną z użyciem procesora FFT w technologii FPGA***)

Keywords: magnetic flux density, fluxgate magnetometer, matched filtering, discrete Fourier transform, FPGA.
Słowa kluczowe: indukcja magnetyczna, magnetometr transduktorowy, filtracja dopasowana, dyskretna transformata Fouriera, FFT, FPGA

Introduction

The automatic detection, identification and measurement of parameters of moving objects is needed in many areas of science and technology. One of the means to reach this aim can be the measurement of the change of magnetic field [1,2]. Every vehicle is built of ferromagnetic components that perturb the uniformity of the Earth magnetic field. This perturbation can be measured with the use of magnetic sensors. The magnetic signals can be distorted by noise. Therefore, before detection and identification the measures to improve the signal-to-noise ratio (SNR) have to be undertaken. These measures may encompass the differential setting of sensors and various kinds of low-pass and band-pass filtering, but the most universal approach seems to be the matched filtering, that allows to reduce wide-band noise. The matched filtering based on the DFT usually requires high-speed signal processing. Such processing can be realized with the use of signal processors or specialized processors implemented inside the Field Programmable Gate Array (FPGA) circuits. Such processors especially in the form of IP Cores, allow for high-speed realization of the Fast Fourier Transform (FFT), which is the main part of the computation procedure.

In this work the measurement system, the realization of the matched filter based on the FFT FPGA processor and the results of simulation and experimental research are presented.

Fluxgate magnetometer subsystem

In this section we shall present the structure of the wireless fluxgate magnetometer [4,5] subsystem that is used for detection and identification of vehicles in the open space. The additional requirement imposed on the system is the operation under any weather conditions in a possibly long time without service. The subsystem has the following functional units: the fluxgate magnetometer block, directional microphones block, control units of fluxgate magnetometers and microphones, wireless data transmission, digital camera, antenna and GPS. In Figure 1 the block scheme of a single set of sensors in which two three-axis fluxgate magnetometers have been used is presented. The applied fluxgate magnetometer by Bartington [8] is shown in Figure 2. The magnetometers working in the differential system allow to measure the differences of the components of magnetic flux density. The differential system reduces the influence of magnetic noise upon the measured quantities. Using the distribution of the differences of components of the magnetic flux density the object can be detected and identified. The task of the set of directional microphones is the measurement of velocity of the detected vehicle in order to obtain the distribution of the differences of the magnetic flux density as the function of displacement. In the unit of sensors the microprocessor will be applied based on the FPGA by Xilinx. This unit will implement the signal processing that allows to detect the object.

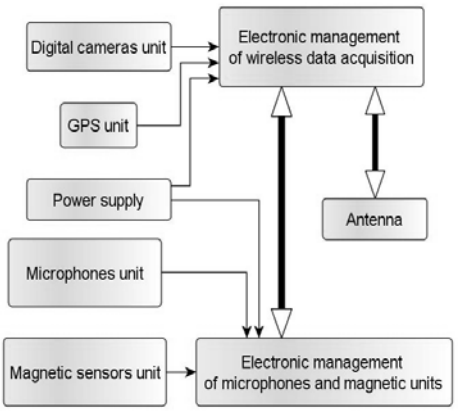

Fig.1. The block scheme of the sensor subsystem

The vehicles to be detected have been divided into four classes: heavy trucks of the TIR type, middle-sized trucks, delivery vans, passenger cars and two-pieces vehicles as the tractor-trailer. The system after detection and identification of the object sends inormation to the wireless transmission unit. The information on the detected object is subsequently sent to the central computer that performs the visualization of the protected area as depicted in Figure 3. Every set of magnetic sensors is equipped with the GPS microchip. This allows to mark precisely the location of

sensors on the map of the protected area. Moreover, due to the use of digital cameras the system operator may require the photograph of the protected area to be sent.

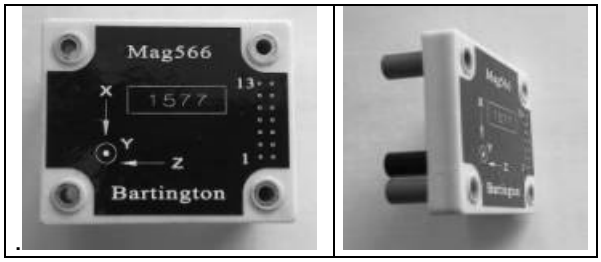

Fig.2. Three-axis transductor magnetometer Mag566 from Bartington

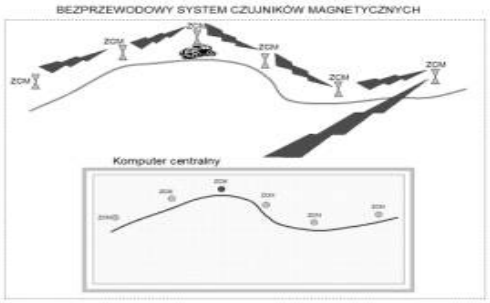

Fig .3. The idea of visualization of the protected area. (ZCM-MSS-magnetic sensor set)

Fig. 4. The placement of the magnetic sensors

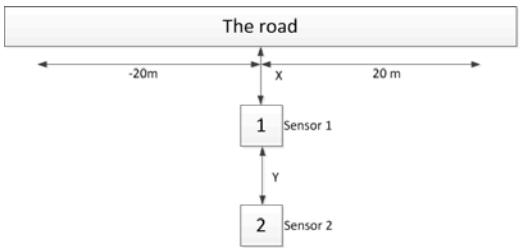

Fig. 5 The scheme of the placement of the magnetic sensors, x - the distance of the sensor 1 from the road and y is the distance between the sensors

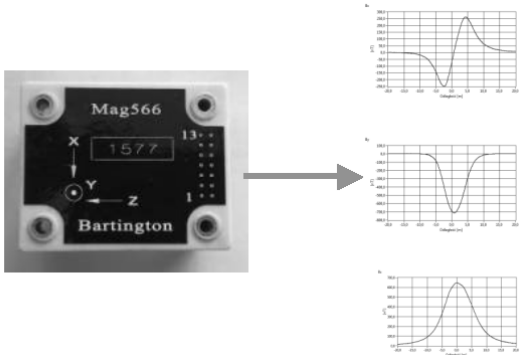

Fig. 5. The measurement unit with 3-axis magnetometer for small magnetic noise

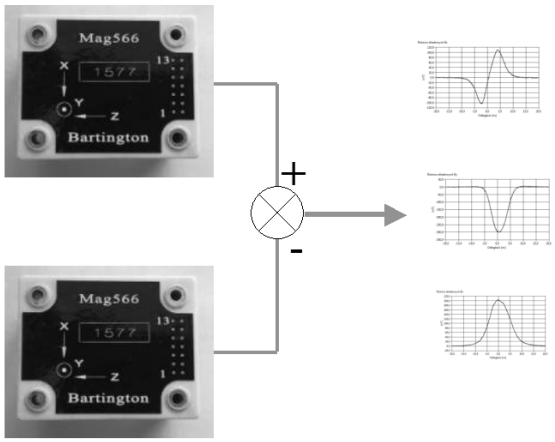

Fig. 6. The measurement unit with two 3-axis magnetometers for large magnetic noise

In Figure 4 the configuration of sensors for two sensors setting is depicted and in Figure 5 the parameters of the placement are shown. In Figures 7-9 we shall present the exemplary screenshots from the measurement system.

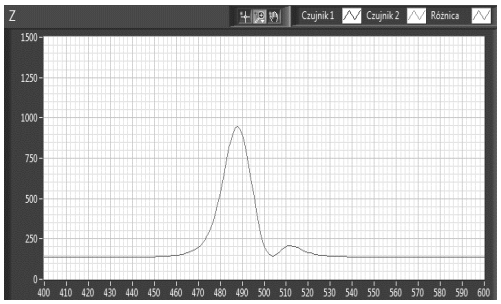

Fig. 7. The distribution of the difference of the component B_z [nT] of the magnetic flux density for a van (x=1 m, y=0,5 m)

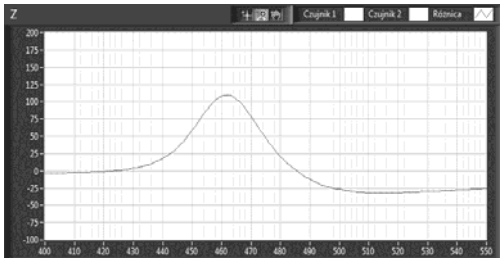

Fig. 8. The distribution of the difference of the component B_z [nT] of the magnetic flux density for a van (x=3,4 m, y=0,5 m)

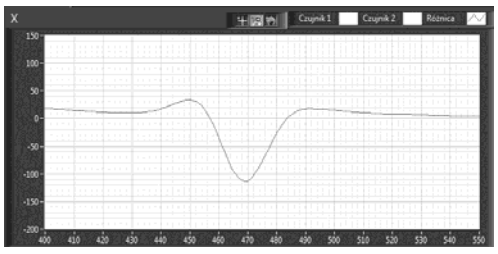

Fig. 9. The distribution of the difference of the component B_x [nT] of the magnetic flux density for a van (x=3,4 m, y=0,5 m)

Mathematical models of the magnetic field of the mechanical vehicles

The mathematical models of the magnetic field of the mechanical vehicles have been prepared with the use of Opera 3D program. In Figure 10 an example of the model of the heavy truck of the TIR type is shown.

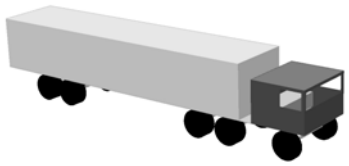

Fig .10. The model of the heavy truck of the TIR type

The numerical analysis of the models of magnetic field of vehicles makes it possible to elaborate the procedures of creating their magnetic signatures.

The choice of location of the vehicle with respect to the Earth magnetic field allows to analyse signals measured by the magnetic sensors for various direction of movements of vehicles. The numerical computations allow for partial analysis of the magnetic field of vehicles because of the limited ability of modeling of the individual parts of the vehicle. This results from the lack of information on permanent magnetism of the ferromagnetic elements of the vehicle. Despite these limitations the numerical simulations allow to perform the qualitative and quantitative analysis of the signals measured with the magnetic sensors in various configurations. In Figure 11 an example of distribution of the modulus of the magnetic flux density in the magnetic direction WE ($y \in <10\ \mathrm{m},\ 20\ \mathrm{m}>$) is presented.

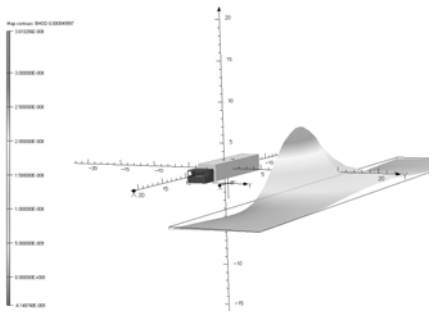

Fig. 11. The distribution of the modulus of the magnetic flux density in the magnetic direction WE ($y \in <10\ \mathrm{m},\ 20\ \mathrm{m}>$).

The modulus of the magnetic flux density has one remarkable extremum. In Figure 12 an example of the distribution of the component B_x of the magnetic flux density of the vehicle in the magnetic direction NS ($y \in <10\ \mathrm{m},\ 20\ \mathrm{m}>$) is depicted. The component B_x has in this case two extrema.

In Figure 13 the distribution of the component B_y in the magnetic direction WE ($y \in <2\ \mathrm{m},\ 20\ \mathrm{m}>$) is shown. The component B_y measured close to the vehicle has two remarkable positive extremal values.

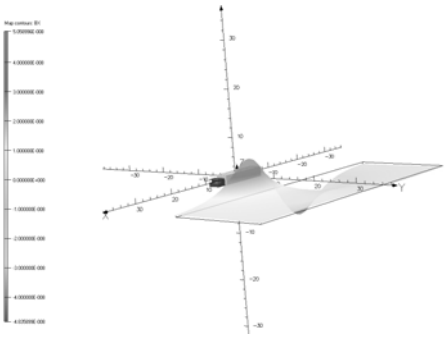

Fig. 12. The distribution of B_x component of the magnetic flux density in the magnetic direction NS ($y \in <10\ \mathrm{m},\ 20\ \mathrm{m}>$)

It can be noted that the modulus of the magnetic flux density and the differences of the measured values have the different distributions in dependence of the direction of movement of the vehicle.

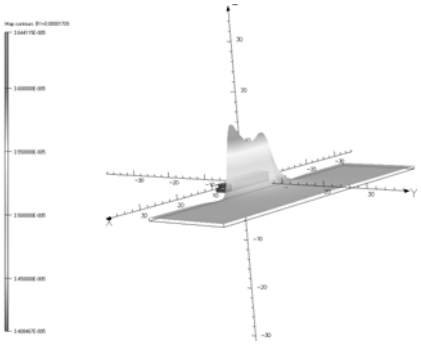

Fig. 13. The distribution of B_y component of the magnetic flux density in the magnetic direction WE ($y \in <2\ \mathrm{m},20\ \mathrm{m}>$)

Experimental results of the measurements

In this section we shall present the selected results of the measurements of magnetic signals from the vehicles. The components of the magnetic flux density were measured for the small van, the truck and the tractor-trailer.

Fig. 14. The object of measurement - the small van

These measurements was made in a forest area, where there was no magnetic noise from the environment. The measurements shown in Figures 15 - 17 have been obtained for the single sensor. This configuration is reasonable for the areas, where the level of the magnetic noise is small. It can be seen that highest values are obtained for the B_z component.

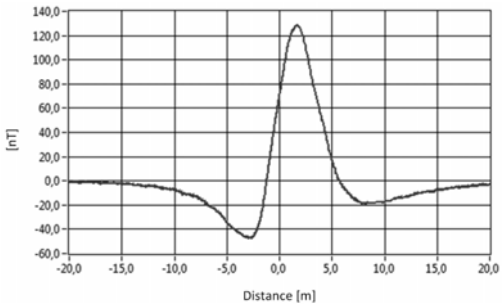

Fig. 15. The distribution of B_x component for the small van in the WE direction

In Figures 19 - 21 the differences of the magnetic flux densities of the individual components are depicted for the truck and in Figures 23 - 25 the respective results for the tractor - trailer are shown. It can be seen that there is the remarkable dependence of the size of the vehicle and the values of the individual components of the magnetic flux density. For example, ΔB_x for the truck is in the range $[-100,100]\,\mathrm{nT}$, whereas for the truck - trailer we have about

$[-45{,}58]\,\mathrm{nT}$. Moreover, the important fact is that if the vehicle consists of two pieces, it is seen in the components ΔB_x and ΔB_y. In this situation we have two extrema indicating the individual pieces of the vehicle. The results of the measurements indicate that not only the detection of the vehicle is posiible but also the identification of the type of the vehicle.

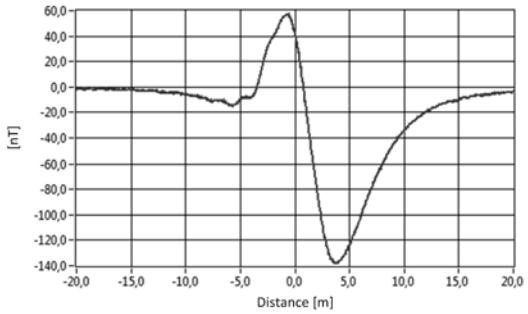

Fig. 16. The distribution of B_y component for the small van in the WE direction

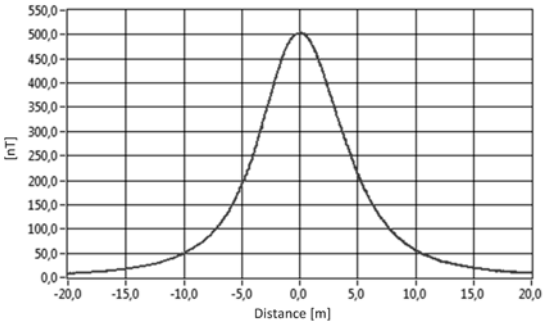

Fig. 17. The distribution of B_z component for the small van in the WE direction

Fig. 18. The object of measurement - the truck

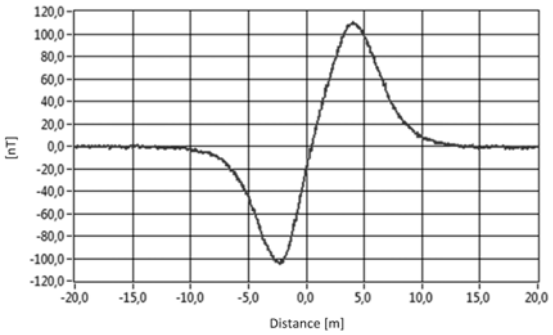

Fig. 19. The distribution of ΔB_x for the truck, in the NS direction

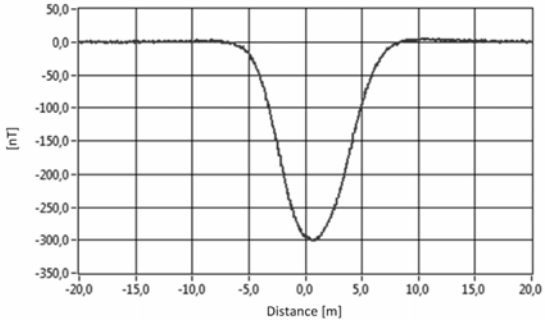

Fig. 20. The distribution of ΔB_y for the truck, in the NS direction

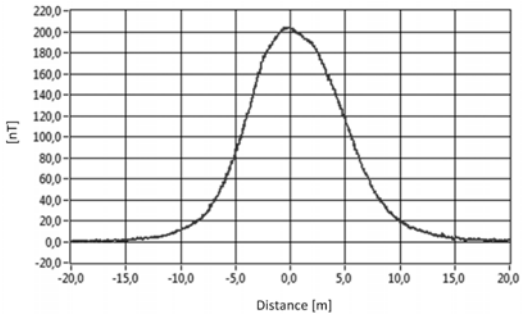

Fig. 21. The distribution of ΔB_z for the truck, in the NS direction

Fig. 22. The object of measurement - the tractor-trailer

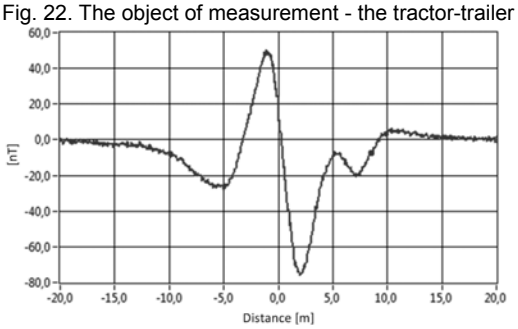

Fig. 23. The distribution of ΔB_x for the tractor-trailer, in the WE direction

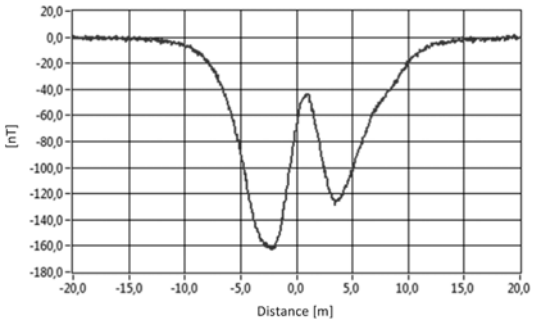

Fig. 24. The distribution of ΔB_y for the tractor-trailer, in the WE direction

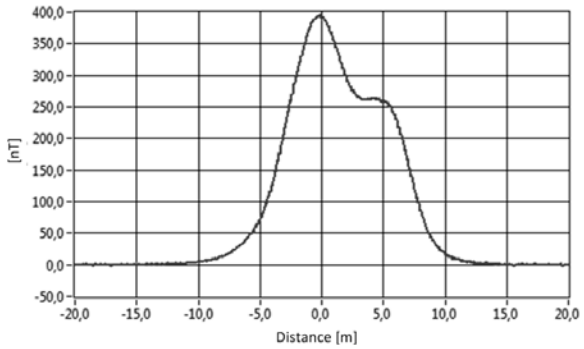

Fig. 25. The distribution of ΔB_z for the tractor-trailer, in the WE direction

Signal denoising by the matched filtering with the FPGA FFT processor

The magnetic signals obtained from the magnetic sensors may be distorted by noise. In order to increase the SNR the matched filter [9] can be applied. The maximum SNR at the matched filter output is obtained when the impulse response of the filter is the time-reversed copy of the input signal. Due to this, the filter maximizes the SNR for the signal being detected in relation to the noise. The filter calculates convolution of the input signal and time-reversed input signal.

The matched filter block diagram is shown in Figure 25. Such filter can be implemented using the Finite Impulse Response (FIR) filter. However, more universal approach can be based on the well-known method of computing the convolution in the frequency domain. This is done by computing the DFT of the input signal, multiplication of the obtained transform by the DFT transform of the impulse response of the filter and next by the performing the inverse DFT transform. This algorithm can be implemented in software or in hardware with the use of specialized FFT processors. Such processors can be implemented using the ASIC approach or by using the FPGA. In the latter case the FFT processor can be realized by using its description in the VHDL or Verilog or by the application of specialized designs supplied by the FPGA manufacturer or by the third party. Such designs are refered to as the IP Core.

The first part of the matched filter is the fixed-point FFT Core [10] that computes the forward DFT. The complex output is multiplied with the use of the complex multiplier in which the matched filter coefficients are multiplied by the DFT samples of the signal to be filtered.

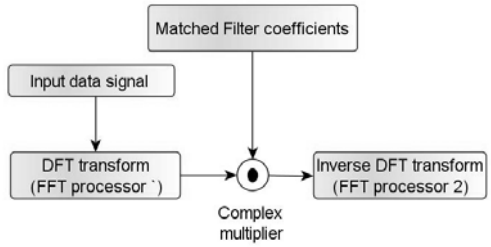

Fig.26. The matched filter block diagram

The FFT core uses the radix-2 butterflies. The core accepts as its input two's complement complex data vector of the variable length from 16 to 16384. The FFT Core outputs the the DFT transform samples in natural order.

Below the synthesis results of the matched filter in the Xilinx environment and the Virtex 5 FPGA circuit are shown.

Selected Device : 5vsx50tff1136-1
Slice Logic Utilization:
Number of Slice Registers: 3261 out of 32640
Number of Slice LUTs: 3024 out of 32640
Number used as Logic: 2122 out of 32640
Number used as Memory: 902 out of 12480
Number used as RAM: 20
Number used as SRL: 882
Timing Summary:
Minimum period: 2,516 ns (Maximum Frequency: 397,456 MHz)
Minimum input arrival time before clock: 2,871 ns
Maximum output required time after clock: 3,344 ns

It is seen that only 10% of the full resouces of the circuit are utilized. The obtained results indicate that the samples can be received with the time rate of about 2,5 ns.

Below in Figures 26-30 the computation results for the van signal are presented.

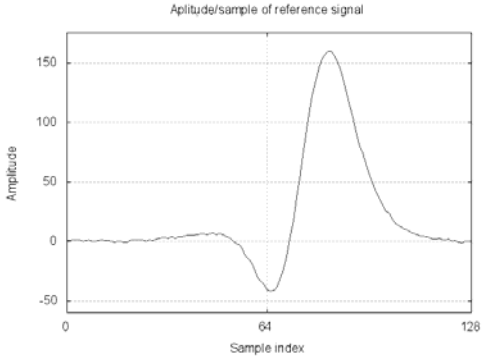

Fig. 27. The reference signal of the van

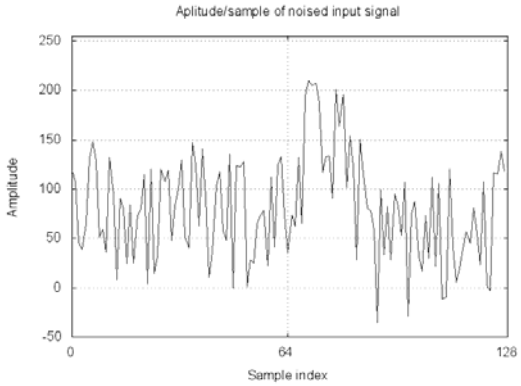

Fig. 28. The noised signal of the van

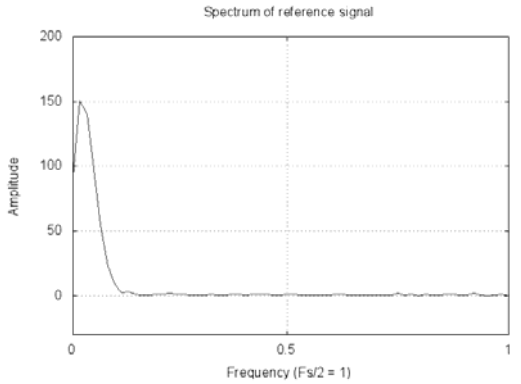

Fig.29. The spectrum of the reference signal

The measured distribution of the differences of the component B_x of the magnetic flux density for the vehicle of van type is shown in Figure 26. In order to examine the effectiveness of denoising procedure, the distorting signal has been added to this signal, and the effect is in Figure 27. The spectrum of the signal without noise is in Figure 28 and the spectrum of the noised signal after filtering in Figure 29. After applying the matched filter the distortions have been effectively limited as it is seen in Figure 30.

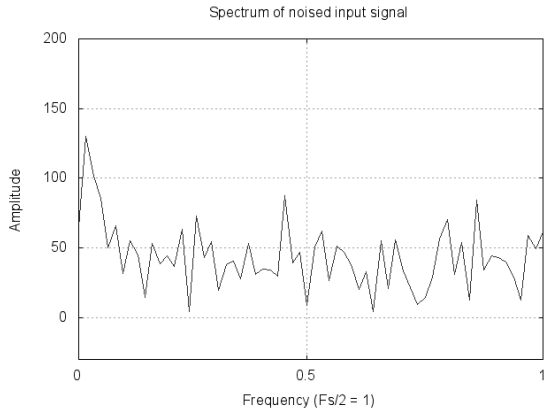

Fig. 30. The spectrum of the noised signal of the van

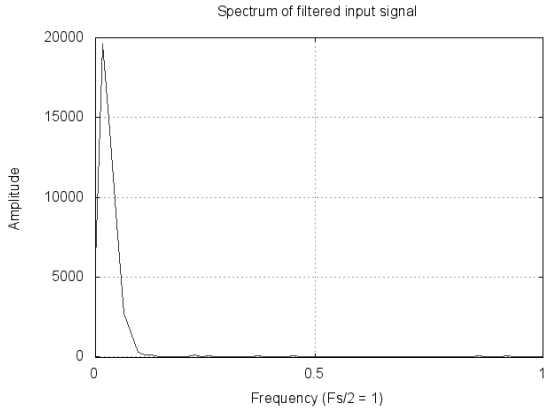

Fig. 31. The spectrum of the noised signal of the van after filtering

Summary

This work presents the measurement system of magnetic signals generated by mechanical vehicles and the denoising procedure and its implementation. The signals are measured with the three-axis fluxgate magnetometers. It has been stated that with the use of the applied magnetometers the detection of the vehicles and identification of the type of the vehicle may be attainable. Generally, the level of the components of magnetic field is proportional to the size of the vehicle, also for the specific vehicles the characteristic features may occur that allow to discriminate one-piece vehicle from the two-piece vehicle. In the noisy environment the measured signalls can be filtered in order to limit the level of the magnetic noise before the detection and identification of the vehicle. In this paper the use of matched filtering in real-time based on the use of the FFT implemented in the Xilinx FPGA has been proposed. The preliminary results suggest the effectiveness of the applied method of denoising of magnetic signals. The future work will encompass the elaboration of algorithms that allow to classify the vehicle.

REFERENCES

[1] Sampey H. R., Vehicle magnetic imaging, (1984) - Numerics, Vanderbilt, PA
[2] The Vehicle Detector Clearinghouse, A Summary of Vehicle Detection and Surveillance Technologies used in Intelligent Transportation Systems (2007)
[3] Marshall S. V., Vehicle Detection Using a Magnetic Field Sensor, *IEEE Trans. Vehicular Technology*, 27, (1978), n.5, 64-68
[4] Caruso M. J., Smith C. H., Schneider R., A New Perspective on Magnetic Field Sensing, 15, (1998) *Sensors Magazine*, n. 12, 34-46
[5] Lenz J. E., A Review of Magnetic Sensors, *Proc. of the IEEE*, 78 (1990), n. 6, 973-989
[6] Ripka P., Review of Fluxgate Sensors, *Sensors and Actuators A*, 33, (1996) 129-141
[7] Ramsden R., Measuring Magnetic Field with Fluxgate Sensors, *Sensors*, (1994) n.9, 87-90
[8] Bartington Instruments, (2012) Mag566 Low Power Three-Axis Magnetic Field Sensor
[9] Richards M. A., Fundamentals of Radar Signal Processing, (2005) McGraw-Hill
[10] Xilinx, LogiCORE IP Fast Fourier Transform v7.1 DS260, (2011) March 1

***Autorzy**: prof. dr hab. inż Kazimierz Jakubiuk, dr inż. Maciej Czyżak, dr inż. Robert Smyk, dr inż. Mirosław Wołoszyn, Politechnika Gdańska, Wydział Elektrotechniki i Automatyki, ul. Narutowicza 11/12 80-266 Gdańsk.*
E-mail: k.jakubiuk@ely.pg.gda.pl; mczyzak@ely.pg.gda.pl; rsmyk@ely.pg.gda.pl; mwolosz@ely.pg.gda.pl.